

# Mitapivat metabolically reprograms human $\beta$ -thalassemic erythroblasts, increasing their responsiveness to oxidation

Angela Siciliano,<sup>1,2</sup> Angelo D'Alessandro,<sup>3</sup> Alessandro Matte,<sup>4</sup> Giovanni Bisello,<sup>5</sup> Mariarita Bertoldi,<sup>5</sup> Monika Dzieciatkowska,<sup>3</sup> Amy Argabright,<sup>3</sup> Richard Huot Pozzetto,<sup>1</sup> Veronica Riccardi,<sup>1</sup> Andrea Mattarei,<sup>6</sup> Alberto Ongaro,<sup>6</sup> Jacopo Ceolan,<sup>1,2</sup> Roberta Russo,<sup>7,8</sup> Leonardo Rivadeneyra,<sup>9</sup> Megan Wind-Rotolo,<sup>9</sup> Achille Iolascon,<sup>7,8</sup> Carlo Brugnara,<sup>10,11</sup> and Lucia De Franceschi<sup>1,2</sup>

<sup>1</sup>Department of Engineering for Innovative Medicine, University of Verona, Verona, Italy; <sup>2</sup>Azienda Ospedaliera Universitaria Integrata, Verona, Italy; <sup>3</sup>Department of Biochemistry and Molecular Genetics, University of Colorado Anschutz Medical Campus, Aurora, CO; <sup>4</sup>Department of Medicine and <sup>5</sup>Department of Neuroscience, Biomedicine and Movement Sciences, University of Verona, Verona, Italy; <sup>6</sup>Department of Pharmaceutical and Pharmacological Sciences, University of Padua, Padua, Italy; <sup>7</sup>Dipartimento di Medicina Molecolare e Biotecnologie Mediche, Università degli Studi di Napoli Federico II, Naples, Italy; <sup>8</sup>CEINGE Biotecnologie Avanzate, Naples, Italy; <sup>9</sup>Agios Pharmaceuticals, Inc, Cambridge, MA; <sup>10</sup>Department of Laboratory Medicine, Boston Children's Hospital, Boston, MA; and <sup>11</sup>Department of Pathology, Harvard Medical School, Boston, MA

## Key Points

- $\beta$ -thal erythroblasts display persistent compensatory expression of PKM2.
- Mitapivat mitigates Cys-oxidative damage to  $\beta$ -thal erythroblast proteins, with normalization of Prdx2 subcellular compartmentalization.

$\beta$ -thalassemia ( $\beta$ -thal) is a worldwide hereditary red cell disorder characterized by severe chronic anemia. Recently, the pyruvate kinase (PK) activator mitapivat has been shown to improve anemia and ineffective erythropoiesis in a mouse model of  $\beta$ -thal and in patients with non-transfusion-dependent thalassemia. Here, we showed that in vitro CD34<sup>+</sup>-derived erythroblasts from patients with  $\beta$ -thal (codb039) are characterized by persistent expression of 2 PK isoforms, PKR and PKM2, compared with healthy cells. Activation of PKR and PKM2 via mitapivat promoted significant metabolic reprogramming of  $\beta$ -thal erythroblasts, resulting in higher levels of high-energy phosphate compounds, including adenosine triphosphate (ATP) and triphosphate nucleoside pools. Proteomics analyses revealed an accumulation of PKR, suggesting a possible beneficial effect of mitapivat on the stability of PKs. Increased ATP availability was accompanied by a higher degree of protein phosphorylation, especially in proteins involved in cell cycle regulation at the transcriptional, translational, and posttranslational levels, supporting the effect of mitapivat on erythroid maturation. Upon treatment with mitapivat,  $\beta$ -thal erythroblasts showed decreased markers of oxidation, including cysteine oxidative posttranslational modifications, downregulation of heat shock protein 70 and peroxiredoxin-2 expression, and normalization of the redox-dependent subcellular distribution of the latter enzyme. Collectively, our data support a protective effect of mitapivat in  $\beta$ -thal erythropoiesis, an effect favored by its activation of persistently expressed PKR and PKM2. In addition to the anticipated benefits on energy metabolism, we report that mitapivat treatment mitigated the oxidative damage in  $\beta$ -thal erythropoiesis, ensuring improved  $\beta$ -thal erythroblast maturation and survival.

Submitted 14 May 2024; accepted 24 February 2025; prepublished online on *Blood Advances* First Edition 14 March 2025. <https://doi.org/10.1182/bloodadvances.2024013591>.

All data are stored in the Nas-Synology-DS216se hard disk, located at the University of Verona, and will be available on request from the corresponding author, Lucia De Franceschi ([lucia.defranceschi@univr.it](mailto:lucia.defranceschi@univr.it)).

The full-text version of this article contains a data supplement.

© 2025 American Society of Hematology. Published by Elsevier Inc. Licensed under Creative Commons Attribution-NonCommercial-NoDerivatives 4.0 International (CC BY-NC-ND 4.0), permitting only noncommercial, nonderivative use with attribution. All other rights reserved.

## Introduction

$\beta$ -thalassemia ( $\beta$ -thal) is a worldwide hereditary red cell disorder, characterized by chronic anemia, related to both reduced red cell life span and ineffective erythropoiesis.<sup>1,2</sup> Chronic transfusion and intensive iron chelation are standard treatments for  $\beta$ -thal syndromes,<sup>1</sup> but new therapeutic options are being developed, including gene therapy<sup>3</sup> and drugs such as luspatercept.<sup>4</sup> Recently, the pyruvate kinase (PK) activator mitapivat has been shown to improve anemia and ineffective erythropoiesis in a mouse model of  $\beta$ -thal and in patients with non-transfusion-dependent thalassemia. Here, we showed that in vitro CD34<sup>+</sup>-derived erythroblasts from patients with  $\beta$ -thal (codb039) are characterized by persistent expression of 2 PK isoforms, PKR and PKM2, compared with healthy cells. Activation of PKR and PKM2 via mitapivat promoted significant metabolic reprogramming of  $\beta$ -thal erythroblasts, resulting in higher levels of high-energy phosphate compounds, including adenosine triphosphate (ATP) and triphosphate nucleoside pools. Proteomics analyses revealed an accumulation of PKR, suggesting a possible beneficial effect of mitapivat on the stability of PKs. Increased ATP availability was accompanied by a higher degree of protein phosphorylation, especially in proteins involved in cell cycle regulation at the transcriptional, translational, and post-translational levels, supporting the effect of mitapivat on erythroid maturation. Upon treatment with mitapivat,  $\beta$ -thal erythroblasts showed decreased markers of oxidation, including cysteine oxidative posttranslational modifications, downregulation of heat shock protein 70 (HSP70) and peroxiredoxin-2 (Prdx2) expression, and normalization of the redox-dependent subcellular distribution of the latter enzyme. Collectively, our data support a protective effect of mitapivat in  $\beta$ -thal erythropoiesis, an effect favored by its activation of persistently expressed PKR and PKM2. In addition to the anticipated benefits on energy metabolism, we report that mitapivat treatment mitigated oxidative damage in  $\beta$ -thal erythropoiesis, ensuring improved  $\beta$ -thal erythroblast maturation and survival.

Pathophysiologic studies have shown that erythroid oxidation plays a key role in the severity of the  $\beta$ -thal hematologic phenotype.<sup>5,6</sup> Indeed, the expression and localization of typical molecular chaperones, such as HSP70, or atypical chaperones, such as Prdx2, play a crucial role in supporting pathologic erythropoiesis and in ensuring erythroid maturation.<sup>6-9</sup> In the context of murine  $\beta$ -thal erythropoiesis, we recently demonstrated a cooperation between Prx2 and Nrf2, transcriptional factors involved in the expression of antioxidant and cytoprotective systems, such as heme-oxygenase-1 (HO-1).<sup>6-9</sup> In addition, nuclear translocation of Prdx2 has been reported to protect against oxidation-induced DNA damage.<sup>10-13</sup>

In  $\beta$ -thal erythroid cells, a highly pro-oxidant environment results in ineffective erythropoiesis, a process in part explained by low ATP and altered activity of key enzymes in the glycolytic pathway.<sup>14-16</sup> PK is crucial in cell ATP production, being the last enzyme in the payoff steps of the glycolytic pathway; as such, PK is important not only for the survival of mature red cells in circulation but also contributes to meet the energetic needs of a metabolically demanding process such as erythropoiesis.<sup>16,17</sup> The PKR isoform is constitutively expressed in erythroid cells, whereas the PKM2 isoform can be induced by oxidative stress or hypoxia.<sup>18-21</sup> The importance of PK in erythroid maturation is also supported by signs of ineffective erythropoiesis in patients with PK deficiency and in

murine models of PK deficiency.<sup>18-22</sup> Recently, the investigational PK activator mitapivat was shown to significantly improve anemia in a  $\beta$ -thal mouse model: specifically, PK activation was beneficial against both ineffective erythropoiesis and chronic hemolysis.<sup>17</sup> Mitapivat significantly reduced oxidation during  $\beta$ -thal mouse erythropoiesis, with an improvement of mitochondrial function and progress in erythroid maturation.<sup>17</sup> Indeed, PK activation in mitochondria-endowed erythroid precursors favors late glycolytic fluxes, which in turn fuels the generation of late glycolytic end products that can sustain the Krebs cycle. Notably, we found that both PKR and PKM2 were expressed at higher values in murine  $\beta$ -thal red cells fractioned according to red cell age vs wild-type controls, whereas PKR, but not PKM2, was observed in healthy erythrocytes.<sup>17</sup> We suggested that this might be compensatory to overcome the severe oxidation of  $\beta$ -thal erythroid cells. As a proof of concept, we tested mitapivat in vitro in CD34<sup>+</sup>-derived erythroblasts from patients with  $\beta$ -thal (cod<sup>b039</sup>). Mitapivat ameliorated the human erythroid cell maturation index and reduced the amount of Annexin-V-positive  $\beta$ -thal erythroblasts.<sup>17</sup> These laboratory studies were also supported by corroborating evidence of improved anemia from a phase 2 study (NCT03692052) in patients with non-transfusion-dependent thalassemia.<sup>23,24</sup>

Here, we studied CD34<sup>+</sup>-derived erythroblasts from either healthy controls (HCs) or patients with  $\beta$ -thal (cod<sup>b039</sup>). We showed a protective effect of mitapivat in  $\beta$ -thal erythropoiesis by targeting both PKR and PKM2 through mechanisms involving beneficial effects on both energy and redox metabolism during  $\beta$ -thal erythropoiesis.

## Methods

### Design of the study

Erythroid cultures obtained from the peripheral blood of 5 different healthy subjects and 5 patients with homozygous  $\beta$ -thal intermedia ( $\beta^{0\text{cod}39}$ ) were analyzed. The study was approved by the Ethical Committee of the Azienda Ospedaliera Integrata Verona, Italy (FGRF13IT), and written informed consent was obtained from patients with  $\beta$ -thal and HCs. Mitapivat (2  $\mu$ M) was added to the cell cultures as previously described.<sup>17</sup>

### In vitro human erythropoiesis

Light-density mononuclear cells were obtained by centrifugation on Lymphoprep density gradient (Nycomed Pharma, Oslo, Norway), as previously described.<sup>17</sup> The CD34<sup>+</sup> cells were positively selected by anti-CD34-tagged magnetic beads (Mini-MACS columns; Miltenyi Biotec, Auburn, CA) according to the manufacturer's protocol, and erythroid precursors were cultured as previously described.<sup>17,25</sup> Details are reported in the supplemental Methods.

### Molecular and immunoblot analysis of human erythroid precursors

A total of 1.5 million erythroblasts were collected, solubilized, and analyzed as previously described.<sup>17</sup> For quantitative real-time polymerase chain reaction, messenger RNA was isolated and reverse transcribed into high-purity complementary DNA using  $\mu$ MACS (Magnetic-Activated Cell Sorting) One-step cDNA Kit (Miltenyi Biotec) according to the manufacturer's instructions.

Details are reported in the supplemental Methods (supplemental Table 1).

## Immunomicroscopy assay

Prdx2 cellular distribution was evaluated in erythroid cells as previously described.<sup>5,6</sup> Details are reported in the supplemental Methods.

## Omics analysis

Metabolomics analyses were performed in cells from 4 patients as previously described.<sup>26,27</sup> Details are reported in the supplemental Methods. Proteomics analyses were performed as described.<sup>28</sup>

## Biochemical studies on recombinant PKLR and PKM isoforms

*Escherichia coli*-expressed recombinant PKLR and PKM isoforms were purchased from R&D Systems Bio-Techne. Details of biochemical studies on PKLR and PKM2 are reported in the supplemental Methods.

## Statistics, data processing, and visualization

Details are reported in the supplemental Methods.

## Results

### $\beta$ -thal erythroblasts display persistent expression of PKM and abnormal metabolomic profile compared with healthy cells

We have recently characterized the maturation profile of healthy and  $\beta$ -thal erythroblasts exposed to mitapivat treatment.<sup>29</sup> The ineffective erythropoiesis of  $\beta$ -thal can be recapitulated in vitro, starting from CD34<sup>+</sup> cells collected from patients with  $\beta$ -thal.<sup>17,25</sup> Compared with healthy cells (Figure 1A; supplemental Figure 1A),  $\beta$ -thal erythroblasts exhibited reduced cell growth and abnormal morphology after 14 days in cell culture (Figure 1A), which corresponds to the late phase of erythropoiesis. We then characterized the expression values of PK isoforms PKLR and PKM, the molecular targets of mitapivat. PKLR gene expression declined during erythroid maturation in both healthy and  $\beta$ -thal erythroblasts (Figure 1B). We found upregulation of PKM gene expression in the late phase of  $\beta$ -thal erythropoiesis (14 days of culture) compared with HCs (Figure 1B). These data were also confirmed at the protein expression level by immunoblot analysis (Figure 1C; supplemental Figure 1B).

Despite the limited blood volume that can be obtained from patients with  $\beta$ -thal, the recent advances in sensitivity of the latest generation Orbitrap and trapped ion mobility mass spectrometers allow for the analysis of samples with low cell counts. By leveraging metabolomics and proteomics approaches (Figures 1D and 2, respectively), we first characterized the baseline differences between  $\beta$ -thal and HC erythroblasts (supplemental Table 2). Significant differences between the 2 groups were noted.  $\beta$ -thal erythroblasts were characterized by significantly lower values of metabolites in the pyrimidine pools (Figure 1D); amino acid values (eg, L-alanine, L-asparagine, glycine, and L-glutamine) and 18-series fatty acids (linoleic and linolenic acid; 18:2; 18:3; Figure 1D). On the contrary, long-chain poly-unsaturated and highly unsaturated fatty acids were enriched in  $\beta$ -thal erythroblasts

(especially arachidonate 20:4; eicosa- and docosa- pentaenoic and hexaenoic, 20:5, 20:6, 22:5; 22:6). Similar trends in enrichment of multiple acyl-carnitines (AcCa 18:0, 18:2, and 20:4) and lipid heads (glycerol 3-phosphate and ethanolamine phosphate) were observed.  $\beta$ -thal erythroblasts were also characterized by higher values of pentose phosphate pathway (PPP) metabolites (pentose phosphate isomers, reduced and oxidized nicotinamide adenine dinucleotide phosphate [NADPH], NAD phosphate, and sedoheptulose phosphate); metabolites involved in redox and glutathione homeostasis (ascorbate, glutamyl-alanine, and taurine); and purines and deamination products (adenosine and hypoxanthine; Figure 1D). Figure 1E provides an overview of glycolysis as a heat map, including the PPP, the Krebs cycle (unlike mature red blood cells, erythroblasts are endowed with functional mitochondria), and the adenylate pools. A clear effect on early glycolysis is seen, with accumulation of hexose phosphate compounds accompanied by an apparent rerouting (as inferred by steady-state values) toward the PPP. Elevated fluxes through the PPP have been previously reported in the context of  $\beta$ -thal due to elevated basal oxidant stress.<sup>14</sup> Notably,  $\beta$ -thal erythroblasts had higher values of phosphoglycerate (2 or 3 isomers combined), suggestive of a potential bottleneck at the PK value. Consistently, downstream of pyruvate, lactate, citrate, fumarate, and malate (erythroblasts are endowed with mitochondria) were also lower in  $\beta$ -thal erythroblasts. Altered redox homeostasis would also contribute to the competition between reduced nicotinamide adenine dinucleotide (NADH)-dependent methemoglobin reductase and lactate dehydrogenase for NADH recycling. In part, this is justifying further decrease in pyruvate conversion to lactate, consistent with prior reports in other hematologic disorders such as glucose 6-phosphate dehydrogenase deficiency.<sup>27,30,31</sup> Results are summarized in the map in Figure 1F.

Proteomics analyses confirmed a significant remodeling of the erythroblast proteome in  $\beta$ -thal (top 500 proteins by *t* test in Figure 2A; zoom in for the top 50 differences in Figure 2B). Results are also shown as a volcano plot in Figure 2C and are provided in tabulated form in supplemental Table 2. Of note, results indicated a significant decrease in arginase 2 (ARG2) and elevation in ARG1 in  $\beta$ -thal erythroblasts (Figure 2B-C). The expression values of the enzyme UDP-N-acetylglucosamine-peptide N-acetylglucosaminyl-transferase (OGT) were higher in  $\beta$ -thal erythroblasts, potentially explaining the lower values of its substrate UDP-N-acetylglucosamine in this group (ie, increased consumption as a function of altered glycosylation processes). Pathway analyses of the proteomic results overall indicate an upregulation of proteins involved in chromatin remodeling and cell cycle (CDK1, CEBPZ, and CENPE, etc) and downregulation of protein phosphorylation pathways in  $\beta$ -thal erythroblasts (Figure 2C; supplemental Figures 2 and 3). Higher values of multiple chaperones were observed in the  $\beta$ -thal group (eg, DNAJA1 in Figure 2C). Consistent with a higher value of oxidative stress in the  $\beta$ -thal erythroblast, all peroxiredoxins were found to be elevated in this group (Figure 2D). As an orthogonal validation of the proteomics data, western blot experiments confirmed higher values of HSP70 and Prdx2 in  $\beta$ -thal erythroblasts than in healthy cells (Figure 2E; supplemental Figure 4). Owing to the role of these enzymes in antioxidant defenses, we then focused on redox modifications to protein cysteine residues, as gleaned by proteomics approaches. Results identified a general increase in overall cysteine oxidation in

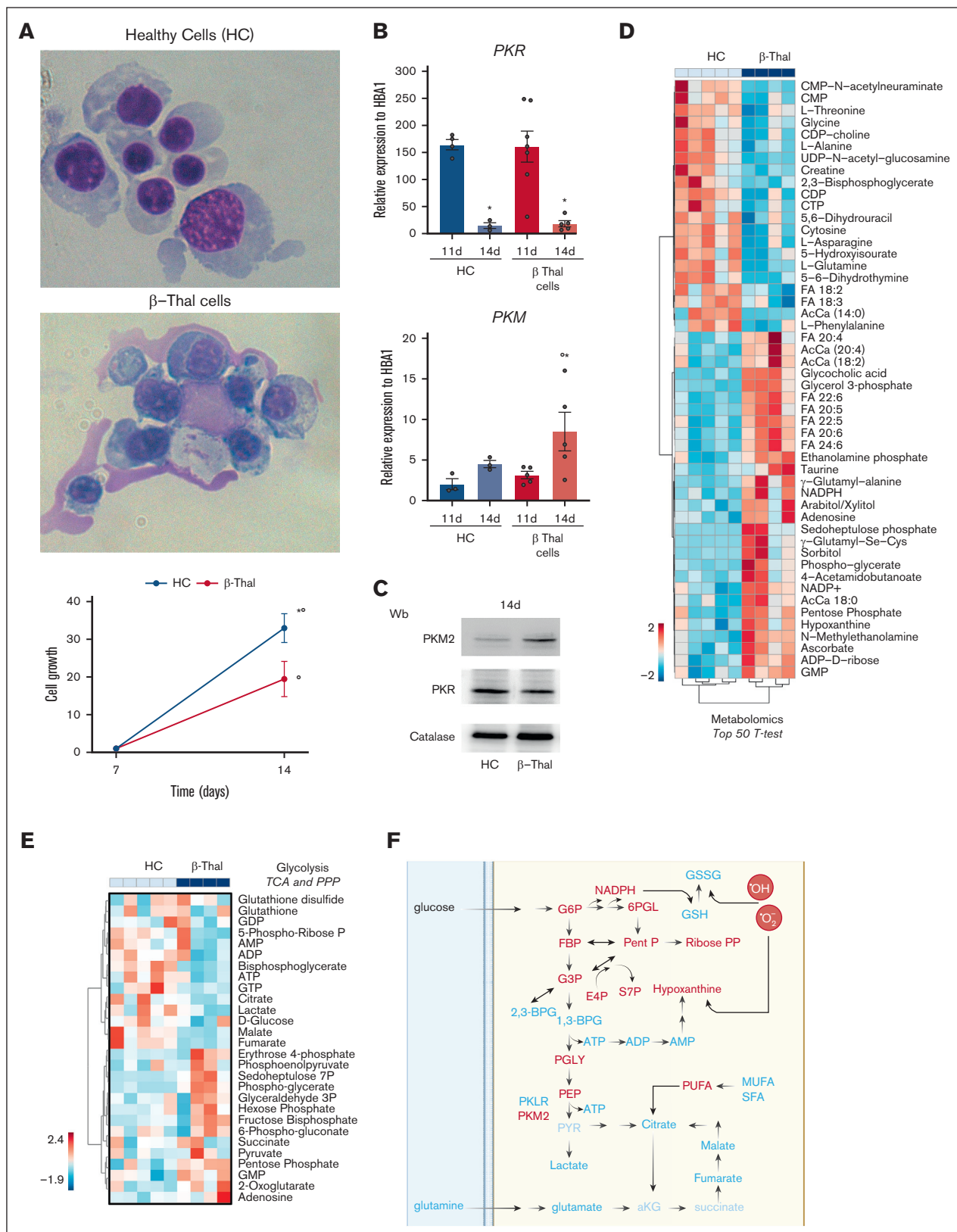


**Figure 1. In vitro  $\beta$ -thal erythroid precursors show reduced cell proliferation, persistence of PKM expression, and abnormal metabolomic and proteomic profiles compared with healthy cells.** (A) May-Grunwald-Giemsa staining for erythroblast morphology (upper) of CD34<sup>+</sup>-derived erythroid precursors on day 14 of culture from HCs and patients with  $\beta$ -thal (cod  $\beta 039$ ) showing irregular nuclear shape and chromatin condensation. One representative image from 5 with similar results is shown. Original



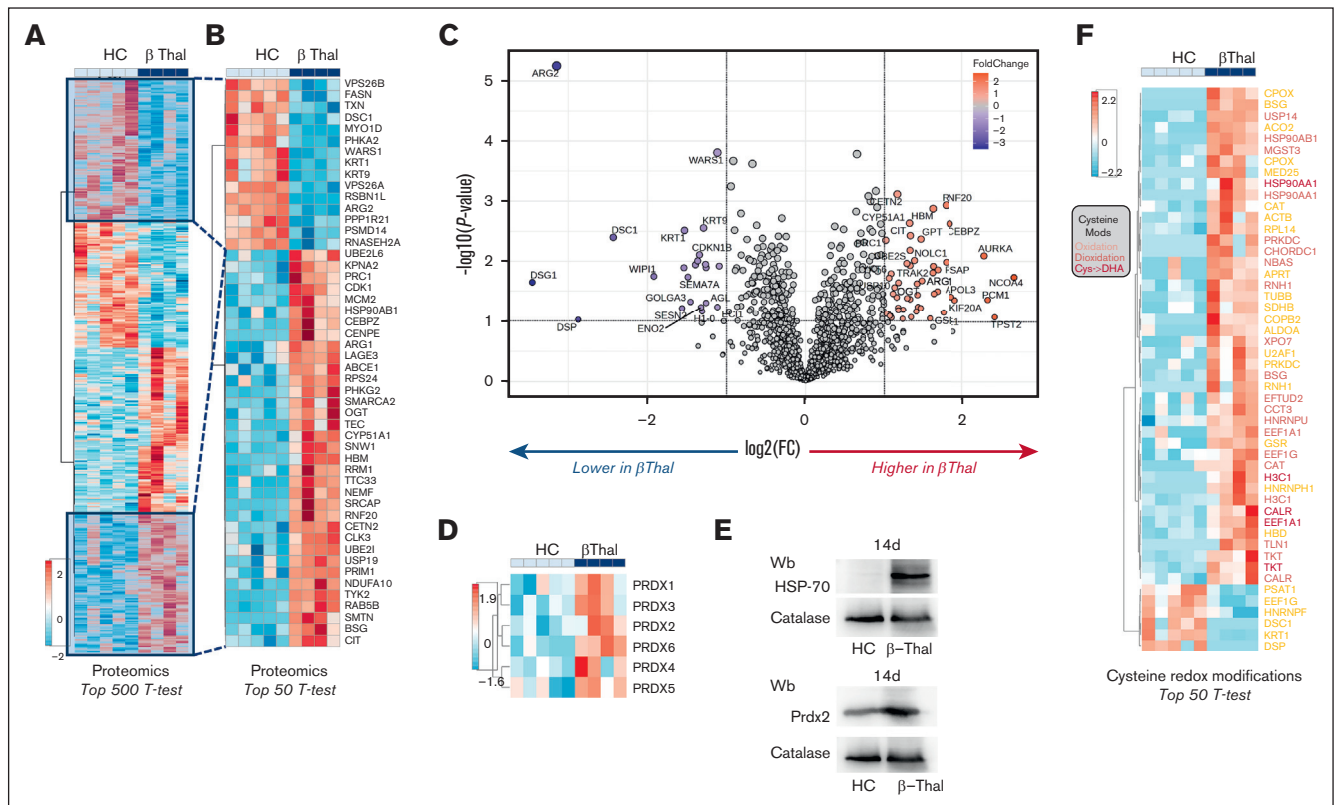


**Figure 2.  $\beta$ -thal erythroblasts are characterized by abnormal proteomic signature and increased overall cysteine oxidation, resulting in upregulation of classic chaperones, such as HSP90 and HSP70, and upregulation of antioxidants, such as peroxiredoxins.** Proteomics profile of erythroid precursors from patients with  $\beta$ -thal vs HCs. Specifically, the heat maps show the top 500 (A) and 50 (B) significant proteins by  $t$  test. (C) The volcano plot indicates proteins whose values are increased (red) or decreased (blue) in  $\beta$ -erythroblasts compared with healthy counterparts. (D) Heat map showing the relative abundance of all peroxiredoxins (Prdx) in the 2 groups. (E) Western blot analysis with specific antibodies against HSP70 and Prdx-2 of erythroid precursors, as in panel A, on day 14 of culture. Catalase was used as loading control. One representative immunoblot of 3 others with similar results. Densitometric analysis is shown in supplemental Figure 2. (F) Heat map showing cysteine redox modifications (colors were coded as follows: oxidation, orange; dioxidation, red; cysteine to dehydroalanine, magenta) between the 2 groups.

$\beta$ -thal erythroblasts compared with HCs, especially oxidation, deoxidation, and, to a lesser extent, irreversible  $\beta$ -elimination of the cysteine thiol group to generate dehydroalanine (Figure 2F). Several antioxidant enzymes (eg, catalase [CAT] and glutathione reductases [Gsr]), chaperones (HSP90AA1 and HSP90AAB1), and metabolic enzymes (aldolase [ALDOA], transketolase [TKT], and succinate dehydrogenase B [SDHB]) were found to be more oxidized at functional cysteine residues in the  $\beta$ -thal group (Figure 2F). For example, deoxidation of Cys101 of SDHB contributes to explaining lower fumarate-to-succinate ratios (Figure 1F) and inferred slower fluxes through mitochondrial electron transport chain complex II,<sup>32</sup> as gleaned from steady-state data.<sup>33</sup> Taken together, our data indicate that in  $\beta$ -thal erythropoiesis, the persistence of PKM2 expression might be compensatory to severe

oxidation of  $\beta$ -thal erythroblasts to ensure cell survival and cell growth. However, it has been extensively shown that PKM2 has slower kinetics than the PKM1 or PKLR isoforms.<sup>34</sup> Therefore, at the metabolic level, these molecular changes translate into the incapacity to maintain comparable pools of late payoff step values of glycolytic metabolites downstream of PK, suggesting that pharmacological interventions could be used to favor ATP synthesis in metabolically challenged  $\beta$ -thal erythroblasts.

## Mitapivat metabolically reprograms human $\beta$ -thal erythroblasts

Early studies have shown that mitapivat increased the activity of both PKR and PKM2 isoforms, resulting in increased ATP.<sup>35,36</sup>

**Figure 1 (continued)** magnification, 100 $\times$ . Quantification of abnormal erythroblasts is shown in supplemental Figure 1A. Cell growth (lower) of the erythroid precursors, as in upper panel. Data are mean  $\pm$  standard error of the mean (SEM;  $n = 5$ ). \* $P < .05$  (compared with HC cells). (B) *PKLR* and *PKM* gene expression normalized on *HBA1* expression (upper) in erythroid precursors on days 11 and 14 of culture from HCs and patients with  $\beta$ -thal. Data are mean  $\pm$  SEM ( $n = 3-5$ ). \* $P < .05$  (compared with 11th day); ° $P < .05$  (compared with HC cells). (C) Western blot analysis with specific antibodies against PKLR and PKM2 of erythroid precursors, as in panel A, on day 14 of culture. Catalase was used as loading control. One representative immunoblot of 3 others with similar results. Densitometric analysis is shown in supplemental Figure 1B. (D) Metabolomics profile of erythroid precursors, after 14 days in culture, from HCs and patients with  $\beta$ -thal (cod  $\beta$ 039). Heat maps show the top 50 significant metabolites (see also supplemental Figure 8). (E) Heat map focusing on glutathione homeostasis, purine metabolites, glycolysis, Krebs cycle (tricarboxylic acid cycle [TCA]), and PPP. (F) A summary overview of the metabolic pathways in panel E; blue-white-red indicate lower to higher values of a given metabolite in  $\beta$ -thal erythroblasts compared with healthy cells.

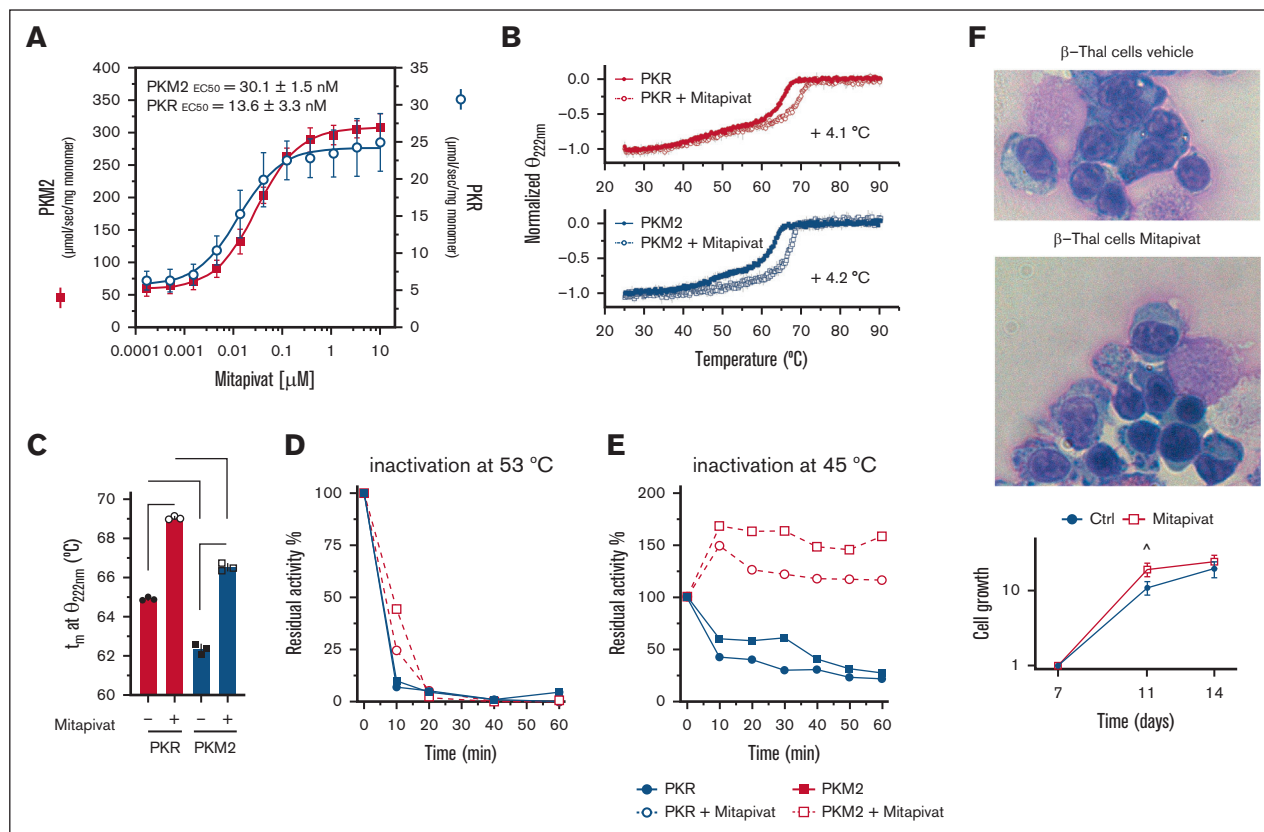


**Figure 3. Mitapivat activates both recombinant PKLR and PKM2, increases protein thermal stability, and ameliorates morphology of  $\beta$ -thal erythroblasts.** (A) In vitro activity of recombinant PKLR and PKM2 enzymes incubated with increasing concentrations of mitapivat. Data are mean  $\pm$  standard deviation (SD;  $n = 3$ ). (B) Dichroic signal (at 222 nm) of thermal denaturation of PKLR and PKM2 recorded in the absence or presence of saturating concentration of mitapivat (10  $\mu$ M). Data are mean  $\pm$  SD ( $n = 3$ ). (C) Comparison between the calculated melting temperatures and statistical analysis. Data are mean  $\pm$  SD ( $n = 3$ ).  $t$  test significance, \*\*\*\* $P \leq 0.0001$ . (D) Residual activity of PKLR and PKM2 enzymes in the absence or presence of mitapivat (10  $\mu$ M) after incubation at 53°C. Values are reported as percentage of the initial activity assayed at 25°C. (E) Residual activity of PKLR and PKM2 at 45°C. All error bars are SDs. (F) May-Grunwald-Giemsa staining for erythroblast morphology (upper) of CD34<sup>+</sup>-derived erythroid precursors, on day 14 of culture, from patients with  $\beta$ -thal (cod  $\beta$ 039) with or without mitapivat, showing improvement of irregular nuclear shape and chromatin condensation. One representative image from 5 with similar results is shown. Original magnification, 100 $\times$ . Quantification of abnormal erythroblasts is shown in supplemental Figure 3A. Cell growth (lower) of the erythroid precursors, as in panel A. Data are mean  $\pm$  SEM ( $n = 5$ ).  $P < .05$  (compared with vehicle-treated cells).

Here, we confirmed the ability of mitapivat to activate both recombinant PKR and PKM2 (Figure 3A). The thermal stability profiles showed that PKR is more stable than PKM2. The binding of mitapivat significantly increases protein stability of both isoforms to approximately the same extent (Figure 3B-C). In addition, mitapivat improved resistance to thermal gradient-induced inactivation for both isoforms (Figure 3D-E), with PKM2 being slightly, even if not significant, more resistant to heat inactivation than PKR, consistent with previous reports.<sup>35,36</sup> Of note, PKM2 recovered a markedly increased activity with respect to PKR (Figure 3E). This unique functional profile of mitapivat, targeting both PK isoforms, might be extremely useful in a model of pathologic erythropoiesis characterized by the persistence of Pkm2 expression, as in  $\beta$ -thal. Indeed, we have previously shown that mitapivat has limited effects on cell growth, but significantly increases  $\beta$ -thal erythroid maturation and reduces the amount of Annexin-V-positive  $\beta$ -thal cells.<sup>17</sup> Here, we confirmed that mitapivat promoted a slight increase in cell growth in treated  $\beta$ -thal cells (Figure 3F). This was associated with an improvement of  $\beta$ -thal erythroblast morphology, as supported by the presence of cells with more regular nuclei and more

condensate chromatin (Figure 3F; supplemental Figure 5A). No major changes in PKLR and PKM gene expression were observed in  $\beta$ -thal with or without mitapivat after 14 days in cell culture (supplemental Figure 5B). Proteomics analyses showed an increase in PKR values but not of PKM proteoforms<sup>37</sup> upon mitapivat treatment (Figure 4A-B). Despite minor inconsistency with the western blot data due to the different technical approach, as shown in Figure 1A-B (ie, similar trends and different level significance), this result is consistent with the thermal protein stability data (Figure 3E). Thus, the accumulation of PKR in mitapivat-treated cells might represent a regulatory mechanism to reach high activity for both protein species. Mitapivat treatment had widespread significant effects on the erythroblast proteome (Figure 4C), promoting decreases in the values of proteins involved in inflammatory pathways (cytokine-mediated signaling) and JAK/STAT cascades (supplemental Figure 6), with concomitant increase in the values of proteins involved in mitophagy and autophagic responses (supplemental Figure 7). Functionally, mitapivat treatment significantly affected the metabolome of  $\beta$ -thal erythroblasts (Figure 4D), with significant upregulation of multiple

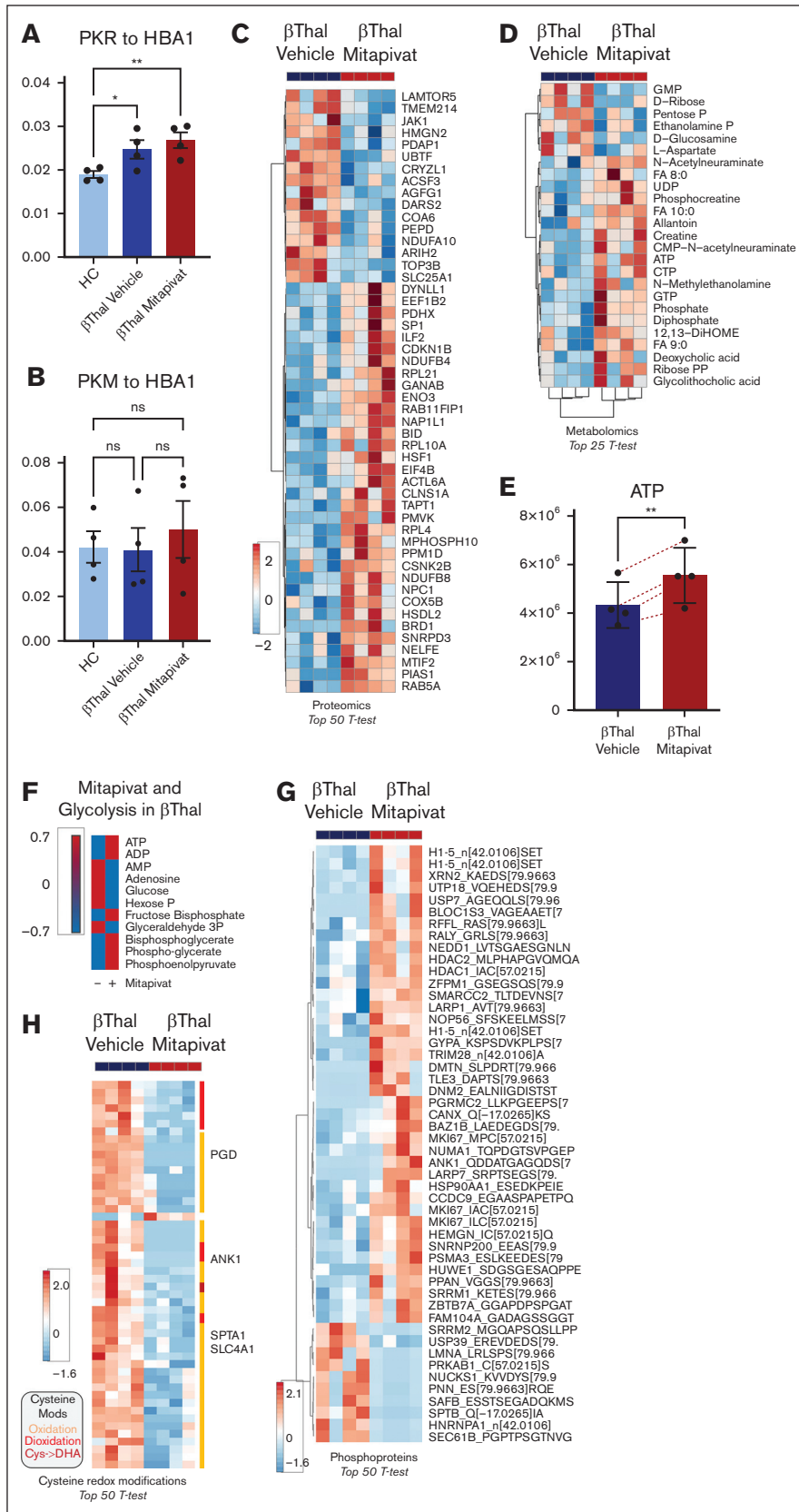


**Figure 4. In vitro, mitapivat ameliorates the metabolic and proteomic profiles of human  $\beta$ -thal erythroblasts, associated with decreased overall cysteine oxidation and downregulation of HSP70 expression.** PK isoforms PKLR (A) and PKM (all proteoforms) (B) in  $\beta$ -thal erythroblasts as a function of mitapivat treatment. (C) Top 50 proteins (by *t* test) affected by mitapivat treatment in  $\beta$ -thal erythroblasts (see also supplemental Figure 9). (D) The heat map shows the metabolites that were significantly (*t* test) affected by mitapivat treatment of  $\beta$ -thal erythroblasts. (E) A detail of ATP, increasing significantly upon mitapivat treatment. (F) Overview of adenylate pools and glycolysis (group averages) in  $\beta$ -thal erythroblasts in the presence or absence of mitapivat (blue vs red indicates low vs high). (G) Elevated ATP values in the mitapivat-treated group corresponded to significant elevation in overall protein phosphorylation. (H) Heat map of the top 50 cysteine redox modifications in  $\beta$ -thal erythroblasts upon mitapivat treatment shows a significant decrease in overall oxidation (orange), deoxidation (red), and cys<math>\rightarrow

high-energy phosphate nucleosides, such as ATP (Figure 4E), CTP, and GTP (Figure 4D). Because we did not observe significant changes in the values of Krebs cycle intermediates, these results are at least in part explained by the decreases in the early and increases in all the late intermediates of glycolysis, suggesting that mitapivat promotes fluxes toward the critical ATP-generating steps of this pathway (Figure 4F). Further studies with stable isotope-labeled substrates (eg, U-<sup>13</sup>C<sub>6</sub>-glucose) will be necessary to test this interpretation of the steady-state data. Specifically, mitapivat activation of PK was accompanied by increases in PGLY:DPG ratios, despite observed increases in the values of both metabolites. Significantly lower values of pentose phosphate compounds (isobaric isomers are unresolved by the high-throughput analytical workflow used here) were observed upon mitapivat treatment (Figure 4D), suggesting a decrease in PPP activation, consistent with decreases in oxidant stress in the mitapivat-treated group. Of note,  $\beta$ -thal erythroblasts are characterized by depletion of all pyrimidine pools, especially cytosine- and uridine-containing metabolites that are involved in sialic acid metabolism and membrane-protein glycosylation. This is relevant in light of the well-established differential glycosylation<sup>38</sup> and sialic acid profiles of abundant erythrocyte membrane proteins (eg, GYPA) in  $\beta$ -thal.<sup>39</sup> Treatment with mitapivat was found to replenish the triphosphate pools for these nucleosides as well.

Increased ATP availability can fuel kinase activity, which in turn could contribute to the widespread proteomics changes observed upon treatment with mitapivat. When focusing on phosphopeptide changes, results show a significant increase in total phosphorylated peptides at serine, threonine, and tyrosine residues in the mitapivat-treated group (Figure 4G). Phosphorylation targets include multiple histones (H1.5 at T11, a marker of mitosis),<sup>40,41</sup> hematopoietic cell growth-regulating factors (hemogen [HEMGN] at S201 and MKI67 at S2105),<sup>42-44</sup> transcriptional/translational regulators (eg, XRN2 and LARP1), and epigenetic regulators (including histone deacetylase 1 [HDAC1] and HDAC2 at functional S421 and S394, respectively, involved in histone complex formation<sup>32</sup> and deacetylase function),<sup>45-47</sup> heat shock proteins (HSP90AA1 at regulatory S263),<sup>48,49</sup> and protein degradation (NEDD8, HUWE1, USP7, and PSMA3) and structural/functional components (glycophorin A [GYPA] at S130; ankyrin [ANK1] at S166; dematin [DMTN] at T274<sup>50</sup>; but not  $\beta$  spectrin [SPTB] at S2114 and T2110<sup>51</sup>; Figure 4G). We show in supplemental Figures 8 and 9 the top 100 identified metabolites and proteins in all 3 different conditions (healthy cells and  $\beta$ -thal cells treated with either vehicle or mitapivat). Altogether, these results in part contribute to bridging the observed metabolic effects of the mitapivat treatment, consistent with its known molecular target PK, and the overall increase in maturation and longevity observed in treated  $\beta$ -thal erythroblasts.

### Mitapivat-treated $\beta$ -thal erythroblasts showed amelioration of cysteine redox proteome oxidation and downregulation of Prdx2 expression toward a normalization of Prdx2 cell distribution

To further expand on the potential benefits of mitapivat on  $\beta$ -thal erythroblasts with respect to the intracellular redox milieu, we performed redox proteomics analyses of  $\beta$ -thal cells as a function of mitapivat treatment (supplemental Table 2; Figure 4H). Results

indicate an overall decrease in total cysteine oxidation, deoxidation, and conversion of cysteine to dehydroalanine (irreversible) in the treated group (heat map in Figure 4H). Specifically, decreases in cysteine oxidation were observed on multiple cysteine residues of several metabolic enzymes (eg, 6-phosphogluconate dehydrogenase [PGD] at C199, in proximity to the active site, and at C422) and structural proteins. The latter group included band 3 (SCL4A1 at C317, functional residue interacting with ankyrin),<sup>52</sup> ANK1 (C864), and SPTA1 (at C965), suggestive of a beneficial effect of mitapivat on membrane protein interactions and stability.<sup>53</sup> Prdx2, one of the more abundant cytoplasmic proteins of erythroid cells, plays an important role in red cells and during erythropoiesis; specifically, Prdx2 acts as an antioxidant, cytoprotective system, and atypical chaperone.<sup>5,6,54,55</sup> As shown in Figure 5A, the improvement in the intracellular milieu of  $\beta$ -thal erythroblasts by mitapivat was also supported by the downregulation of *PRDX2* and *HMOX1* (heme-oxygenase-1) gene expression after 14 days in cell culture (Figure 5A; supplemental Figure 10A). Both systems were upregulated at both gene and protein levels in response to oxidative stress in vehicle-treated  $\beta$ -thal erythroblasts, in agreement with prior studies by our group on erythroid precursors (Figure 5A-B; supplemental Figure 10A-B).<sup>6,17,54</sup> Previous reports in different cell types, such as cancer cell lines or neurons, have shown that differences in the compartmental distribution of Prdx2 between cytoplasm and nucleus affect the role of enzyme as a protective agent against oxidation-induced DNA damage.<sup>10-13</sup> When we evaluated Prdx2 localization in  $\beta$ -thal erythroid precursors, we observed a differential localization as a function of mitapivat treatment. As shown in Figure 5C, Prdx2 distribution was essentially cytoplasmic in healthy cells, whereas Prdx2 had cytoplasmic and nuclear compartmentalization in  $\beta$ -thal cells treated with vehicle, compared with healthy cells. Mitapivat treatment reduced Prdx2 expression (Figure 5B; supplemental Figure 10B) and normalized Prdx2 localization in  $\beta$ -thal cells compared with vehicle-treated  $\beta$ -thal erythroblasts (Figure 5C). In mitapivat-treated  $\beta$ -thal erythroblasts, the expression of HSP70 significantly decreased, reaching values similar to healthy cells, compared with vehicle-treated  $\beta$ -thal erythroid cells (supplemental Figure 10C).

## Discussion

In the context of in vitro human  $\beta$ -thal erythropoiesis, we have previously reported that mitapivat improves the erythroid maturation index and reduces the amount of Annexin-V–positive cells.<sup>17</sup> Here, we show that mitapivat, which targets both PKR and PKM2 isoforms, metabolically reprograms  $\beta$ -thal erythroblasts, favoring late glycolysis, which in turn boosts adenylate pools and promotes regulatory protein phosphorylation to enhance cell maturation and growth. Indeed, we found a persistent expression of PKM2 during  $\beta$ -thal erythropoiesis compared with healthy erythroblasts. Papoin et al recently reported a progressive downregulation of PKM2 expression from early to late stages of maturation in healthy human erythroid progenitor cells, suggesting PKR to be the dominant PK isoform in healthy erythroid progenitors entering the late stage of erythropoiesis.<sup>56</sup> In human  $\beta$ -thal, we propose that the persistence of PKM2 expression mitigates the metabolic perturbations associated with severe oxidation in  $\beta$ -thal erythroblasts, mainly related to the intracellular pro-oxidant environment. This adaptation holds some relevant metabolic implications, owing to the redox sensitivity of PKM2,<sup>57</sup> an important caveat in  $\beta$ -thal erythroblasts, in which



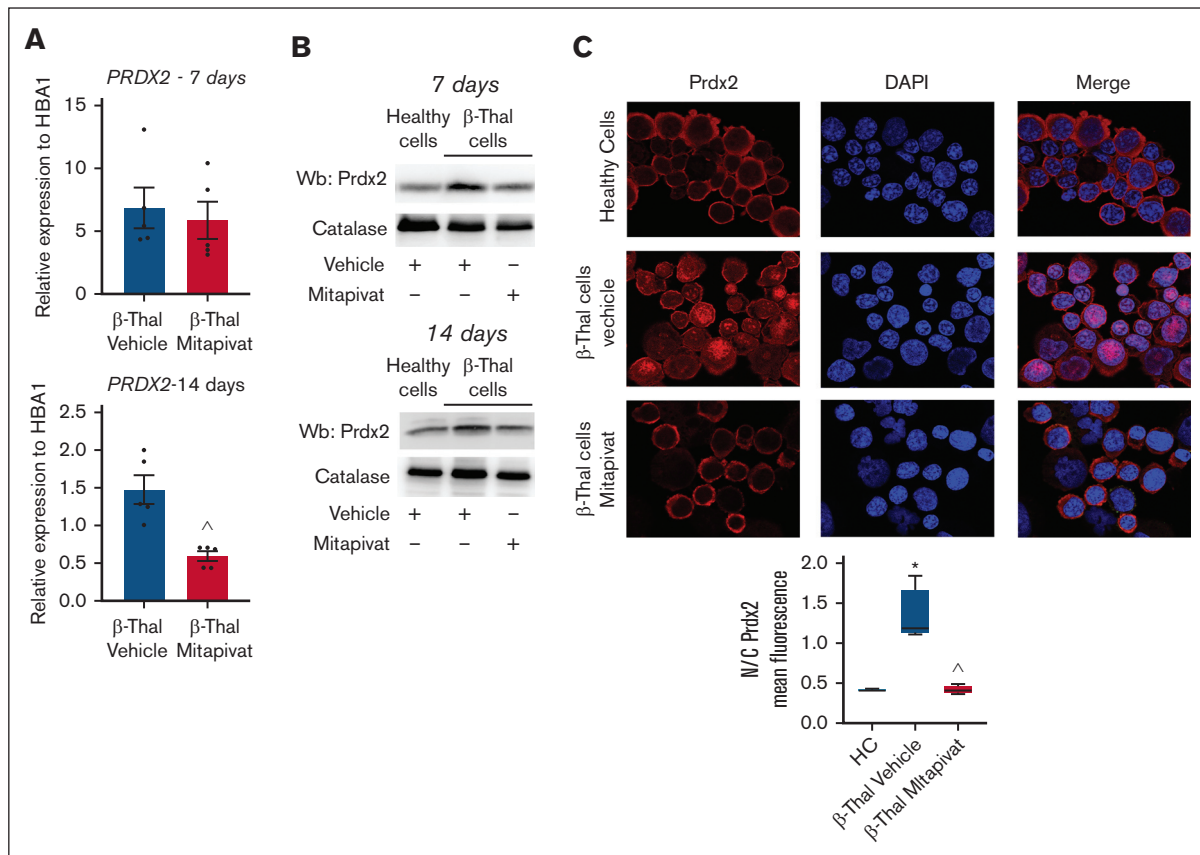


**Figure 5. In  $\beta$ -thal erythroblasts, mitapivat normalizes the stress-induced upregulation and nuclear recruitment of Prx-2.** (A) *PRDX2* gene expression normalized on *HBA1* expression in  $CD34^+$ -derived erythroid precursors, on days 7 (upper) and 14 (lower) of culture, from patients with  $\beta$ -thal (cod  $\beta 039$ ) in vitro treated with vehicle or mitapivat (2  $\mu$ M). Data are mean  $\pm$  SEM ( $n = 5$ );  $P < .05$  (compared with vehicle-treated cells). (B) Western blot analysis of Prdx2 in erythroid precursors, as in panel A. Catalase served as loading controls. One representative immunoblot of other 4 with similar results. (C) Prdx2 immunostaining of  $CD34^+$ -derived erythroid precursors from HC and patients with  $\beta$ -thal (cod  $\beta 039$ ) in vitro treated with vehicle or mitapivat (2  $\mu$ M). DAPI (4',6-diamidino-2-phenylindole) was used to stain nuclei. Prx2 mean fluorescence in the nucleus and cytoplasm was measured using ImageJ. Four different squares and at least 150 cells were analyzed. Data are presented as median and minimum/maximum, with boxes indicating 25th to 75th percentiles;  $*P < .05$  (compared with HC);  $^{\wedge}P < .05$  (compared with vehicle-treated cells).

basal values of oxidant stress are higher than in HCs. Depletion of glutathione pools and elevation in the expression values and cellular compartmentalization of all peroxiredoxins, especially Prdx2, support the severe and sustain pro-oxidant environment of  $\beta$ -thal erythroblasts. This agrees with our previous reports showing the important cytoprotective and adaptogenic role of Prdx2 against oxidation in  $\beta$ -thal ineffective erythropoiesis.<sup>6</sup>

Metabolically, mitapivat sustains an upregulation of fluxes of late glycolytic steps with increased ATP content, ensuring cell survival associated with the activation of protein networks involved in chromatin remodeling (supplemental Figure 2) and cell signaling toward cell maturation. Indeed, we observed increased phosphorylation state of multiple targets of cell cycle-regulating kinases, such as phosphorylation of H1.5 at T11, affecting its nuclear localization.<sup>40,58</sup> We also observed increases in phosphorylation of HEMG, a regulator of stem cell proliferation via control of STAT1 phosphorylation status,<sup>46</sup> and MKI67 (also known as KI-67 proliferation antigen),<sup>59</sup> which is consistent with a role of mitapivat in promoting erythroblast maturation. Similarly, casein kinase II targets HDAC1 and HDAC2 are phosphorylated as a function of oxidant stress<sup>45</sup> and proliferation state.<sup>60,61</sup> Phosphorylation of structural

proteins such as GYPA (at S130), ANK1 (at S166), or DMTN (at T274,<sup>62</sup> a target of PKA activity) may be one of the metabolic benefits of mitapivat, which leads to improved erythroid maturation compared with vehicle-treated cells. On the contrary, 2 of the 4 common phosphorylation sites for SPTB (S2114 and T2110)<sup>51</sup> were found to be less phosphorylated in the  $\beta$ -thal group, suggesting a finely tuned regulation of specific kinase pathways, such as PKA and casein kinase 2, rather than a general upregulation of all phosphorylation events. This is extremely interesting because previous reports have shown that improvements in intracellular cell signaling pathways intersecting EPO-STAT cascade support erythroid maturation.<sup>63-65</sup>

Another piece of evidence of the beneficial effect of mitapivat on cellular function and signaling is the modulation of autophagy-related proteins, which are involved in one of the key adaptive mechanisms to ensure cell survival. Indeed, previous reports linked impairment of autophagy to ineffective erythropoiesis.<sup>66-69</sup> Mitapivat-treated human  $\beta$ -thal cells display activation of mitophagy/autophagy protein networks (supplemental Figure 7). This agrees with our previous report on  $\beta$ -thal mice treated with mitapivat showing improved mitophagy and increased mitochondrial

biogenesis in sorted mouse  $\beta$ -thal erythroid precursors.<sup>17</sup> The functional amelioration of the mitochondrial compartment contributes to the decreased oxidation observed in mitapivat-treated human  $\beta$ -thal cells compared with vehicle-treated cells. Indeed, mitapivat-treated  $\beta$ -thal cells display (1) lower values of oxidant stress, as gleaned by decreased rerouting of glucose oxidation fluxes to the PPP<sup>14</sup>; and (2) decreased overall cysteine oxidation. In agreement, we found downregulation of classical chaperone HSP70 and Prdx2 expression compared with vehicle-treated  $\beta$ -thal cells. In addition, mitapivat-treated  $\beta$ -thal cells display Prdx2 cellular distribution similar to that of healthy erythroblasts, characterized more by cytoplasmic than nuclear localization. Recent reports show that Prdx2 might translocate into the nucleus, bind to the promoter regions of ARE genes, and protect erythroblasts from DNA-damaging oxidation related to aging or radiation.<sup>5,70,71</sup> The amelioration of intracellular environment of mitapivat-treated  $\beta$ -thal erythroblasts is also supported by the reduction in the expression of HO-1, which is a Nrf2-dependent cytoprotective system involved in heme catabolism.<sup>25,55</sup> This is consistent with our previous observation of a functional interplay between Prdx2 and Nrf2, cooperating against oxidation during stress erythropoiesis.<sup>6</sup> Of note, Nrf2 might also modulate the expression of HSP70.<sup>72</sup> Thus, in  $\beta$ -thal erythroblasts, mitapivat metabolically reprograms  $\beta$ -thal cells and attenuates oxidation, preventing the induction of protective mechanisms such as Prdx2 and HSP70.

Although our data shed new light on the effects of mitapivat on human  $\beta$ -thal erythropoiesis, our study has 2 limitations that could be addressed in future studies. The first one is the cell model. Although it recapitulates in vivo human erythropoiesis and our proteomic/metabolomic profile of normal erythroblasts is similar to that reported in erythroid cells from bone marrow of healthy donors,<sup>73-75</sup> future studies might be designed to profile metabolome from bone marrow cells of patients with  $\beta$ -thal. The second limitation concerns the observation on HSP70. Further studies will be conducted to evaluate HSP70 compartmentalization, HSP70 cochaperones, and their link to Nrf2 in mitapivat-treated  $\beta$ -thal erythroblasts.

In conclusion, although caveats are noted owing to the focus on ex vivo models rather than primary in vivo cells, our data show that both PKR and PKM2 isoforms are expressed in the late phase of  $\beta$ -thal erythropoiesis. The ability of mitapivat to stabilize and activate both isoforms might represent an unanticipated benefit of mitapivat treatment, favoring energy metabolism, mitigating oxidant stress in

$\beta$ -thal erythroblasts, and, ultimately, promoting cell maturation and growth.

## Acknowledgments

A.D. was supported by funds by the National Heart, Lung, and Blood Institute (R01HL146442, R01HL149714, R01HL148151, and R01HL161004). This research was funded by Ministero dell'Università e della Ricerca PRIN2020-MIUR (2020Z22PM7) (L.D.F. and A.I.) and supported by Agios collaborative research grant (L.D.F.).

The content is solely the responsibility of the authors and does not necessarily represent the official views of the National Institutes of Health.

## Authorship

Contribution: L.D.F., M.D., A.A., A.D., and A. Matte. generated data; L.D.F., A.D., and M.B. analyzed the data; L.D.F. and M.D. analyzed the omics; A.D. prepared the figures; C.B., L.D.F., and A.D. wrote the manuscript; A.S. and V.R. performed cell cultures; M.B. and G.B. performed in vitro PKLR/PKM2 experiments; A.I., J.C., A.O., L.R., A. Mattarei, and M.W.-R. critically revised the manuscript; A. Matte. and R.H.P. performed cytofluorimetric, immunomicroscopic, and immunoblot analyses; and R.R. performed molecular analyses, analyzed the data, and wrote the manuscript.

Conflict-of-interest disclosure: A.D. is a founder of Omix Technologies Inc, and is also a scientific advisory board member of Hemanext Inc and Macopharma Inc. L.R. and M.W.-R. are employees and shareholders of Agios Pharmaceuticals. L.D.F. received an Agios research grant. The remaining authors declare no competing financial interests.

ORCID profiles: A.D., 0000-0002-2258-6490; G.B., 0000-0002-3803-9555; M.B., 0000-0002-2337-9928; A.A., 0009-0002-1674-0997; V.R., 0000-0002-1845-2553; A.M., 0000-0002-2023-0749; A.O., 0000-0002-8661-2416; A.I., 0000-0002-9558-0356; C.B., 0000-0001-8192-8713; L.D.F., 0000-0001-7093-777X.

Correspondence: Lucia De Franceschi, Department of Engineering for Innovation Medicine, University of Verona & AOUI Verona, P.le L. Scuro, 10, 37134 Verona, Italy; email: [lucia.defranceschi@univr.it](mailto:lucia.defranceschi@univr.it).

## References

1. Taher AT, Musallam KM, Cappellini MD. beta-Thalassemias. *N Engl J Med*. 2021;384(8):727-743.
2. Rivella S.  $\beta$ -thalassemias: paradigmatic diseases for scientific discoveries and development of innovative therapies. *Haematologica*. 2015;100(4):418-430.
3. Locatelli F, Thompson AA, Kwiatkowski JL, et al. Betibeglogene autotemcel gene therapy for non-beta(0)/beta(0) genotype beta-thalassemia. *N Engl J Med*. 2022;386(5):415-427.
4. Cappellini MD, Viprakasit V, Taher AT, et al. A phase 3 trial of luspatercept in patients with transfusion-dependent beta-thalassemia. *N Engl J Med*. 2020;382(13):1219-1231.
5. Matte A, De Falco L, Federti E, et al. Peroxiredoxin-2: a novel regulator of iron homeostasis in ineffective erythropoiesis. *Antioxid Redox Signal*. 2018;28(1):1-14.
6. Matte A, De Falco L, Iolascon A, et al. The interplay between peroxiredoxin-2 and nuclear factor-erythroid 2 is important in limiting oxidative mediated dysfunction in  $\beta$ -thalassemic erythropoiesis. *Antioxid Redox Signal*. 2015;23(16):1284-1297.

7. Matte A, Recchiuti A, Federti E, et al. Resolution of sickle cell disease-associated inflammation and tissue damage with 17R-resolvin D1. *Blood*. 2019;133(3):252-265.
8. Mathangasinghe Y, Fauvet B, Jane SM, Goloubinoff P, Nillegoda NB. The Hsp70 chaperone system: distinct roles in erythrocyte formation and maintenance. *Haematologica*. 2021;106(6):1519-1534.
9. Dussiot M, Maciel TT, Fricot A, et al. An activin receptor IIA ligand trap corrects ineffective erythropoiesis in  $\beta$ -thalassemia. *Nat Med*. 2014;20(4):398-407.
10. Ishii T, Warabi E, Yanagawa T. Novel roles of peroxiredoxins in inflammation, cancer and innate immunity. *J Clin Biochem Nutr*. 2012;50(2):91-105.
11. Lee KW, Lee DJ, Lee JY, Kang DH, Kwon J, Kang SW. Peroxiredoxin II restrains DNA damage-induced death in cancer cells by positively regulating JNK-dependent DNA repair. *J Biol Chem*. 2011;286(10):8394-8404.
12. Park J, Lee S, Lee S, Kang SW. 2-cys peroxiredoxins: emerging hubs determining redox dependency of Mammalian signaling networks. *Int J Cell Biol*. 2014;2014:715867.
13. Mullen L, Hanschmann EM, Lillig CH, Herzenberg LA, Ghezzi P. Cysteine oxidation targets peroxiredoxins 1 and 2 for exosomal release through a novel mechanism of redox-dependent secretion. *Mol Med*. 2015;21(1):98-108.
14. Ting YL, Naccarato S, Qualtieri A, Chidichimo G, Brancati C. In vivo metabolic studies of glucose, ATP and 2,3-DPG in  $\beta$ -thalassaemia intermedia, heterozygous  $\beta$ -thalassaemic and normal erythrocytes:  $^{13}\text{C}$  and  $^{31}\text{P}$  MRS studies. *Br J Haematol*. 1994;88(3):547-554.
15. Chakraborty I, Mishra R, Gachhui R, Kar M. Distortion of  $\beta$ -globin chain of hemoglobin alters the pathway of erythrocytic glucose metabolism through band 3 protein. *Arch Med Res*. 2012;43(2):112-116.
16. Zhang Z, Deng X, Liu Y, Liu Y, Sun L, Chen F. PKM2, function and expression and regulation. *Cell Biosci*. 2019;9:52.
17. Matte A, Federti E, Kung C, et al. The pyruvate kinase activator mitapivat reduces hemolysis and improves anemia in a beta-thalassemia mouse model. *J Clin Invest*. 2021;131(10):e144206.
18. Klei TRL, Kheradmand Kia S, Veldhuis M, et al. Residual pyruvate kinase activity in PKLR-deficient erythroid precursors of a patient suffering from severe haemolytic anaemia. *Eur J Haematol*. 2017;98(6):584-589.
19. Aizawa S, Kohdera U, Hiramoto M, et al. Ineffective erythropoiesis in the spleen of a patient with pyruvate kinase deficiency. *Am J Hematol*. 2003;74(1):68-72.
20. Aizawa S, Harada T, Kanbe E, et al. Ineffective erythropoiesis in mutant mice with deficient pyruvate kinase activity. *Exp Hematol*. 2005;33(11):1292-1298.
21. Max-Audit I, Kechemir D, Mitjavila MT, Vainchenker W, Rotten D, Rosa R. Pyruvate kinase synthesis and degradation by normal and pathologic cells during erythroid maturation. *Blood*. 1988;72(3):1039-1044.
22. Zaninoni A, Marra R, Fermo E, et al. Evaluation of the main regulators of systemic iron homeostasis in pyruvate kinase deficiency. *Sci Rep*. 2023;13(1):4395.
23. Kuo KHM, Layton DM, Lal A, et al. Safety and efficacy of mitapivat, an oral pyruvate kinase activator, in adults with non-transfusion dependent alpha-thalassaemia or beta-thalassaemia: an open-label, multicentre, phase 2 study. *Lancet*. 2022;400(10351):493-501.
24. Ali T, Taher HA-S, Aydinok Yesim, et al. *ENERGIZE: a global phase 3 study of mitapivat demonstrating efficacy and safety in adults with alpha- or beta-non-transfusion-dependent thalassemia*. Madrid, Spain: Paper presented at: European Hematology Association (EHA) Hybrid Congress; 13-16 June 2024.
25. Matte A, Federti E, Winter M, et al. Bitopertin, a selective oral GLYT1 inhibitor, improves anemia in a mouse model of  $\beta$ -thalassemia. *JCI Insight*. 2019;4(22):e130111.
26. Nemkov T, Reisz JA, Gehrke S, Hansen KC, D'Alessandro A. High-throughput metabolomics: isocratic and gradient mass spectrometry-based methods. *Methods Mol Biol*. 2019;1978:13-26.
27. D'Alessandro A, Le K, Lundt M, et al. Functional and multi-omics signatures of mitapivat efficacy upon activation of pyruvate kinase in red blood cells from patients with sickle cell disease. *Haematologica*. 2024;109(8):2639-2652.
28. Thomas T, Stefanoni D, Dzieciatkowska M, et al. Evidence of structural protein damage and membrane lipid remodeling in red blood cells from COVID-19 patients. *J Proteome Res*. 2020;19(11):4455-4469.
29. Matte A, Kosinski PA, Federti E, et al. Mitapivat, a pyruvate kinase activator, improves transfusion burden and reduces iron overload in beta-thalassemic mice. *Haematologica*. 2023;108(9):2535-2541.
30. Nemkov T, Stephenson D, Earley EJ, et al. Biological and genetic determinants of glycolysis: phosphofructokinase isoforms boost energy status of stored red blood cells and transfusion outcomes. *Cell Metab*. 2024;36(9):1979-1997.e1913.
31. Tzounakas VL, Kriebardis AG, Georgatzakou HT, et al. Glucose 6-phosphate dehydrogenase deficient subjects may be better "storers" than donors of red blood cells. *Free Radic Biol Med*. 2016;96:152-165.
32. Saxena N, Maio N, Crooks DR, et al. SDHB-deficient cancers: the role of mutations that impair iron sulfur cluster delivery. *J Natl Cancer Inst*. 2016;108(1):djv287.
33. Jones CL, Stevens BM, D'Alessandro A, et al. Cysteine depletion targets leukemia stem cells through inhibition of electron transport complex II. *Blood*. 2019;134(4):389-394.
34. Caruso P, Dunmore BJ, Schlosser K, et al. Identification of microRNA-124 as a major regulator of enhanced endothelial cell glycolysis in pulmonary arterial hypertension via PTBP1 (polypyrimidine tract binding protein) and pyruvate kinase M2. *Circulation*. 2017;136(25):2451-2467.

35. Rab MAE, Van Oirschot BA, Kosinski PA, et al. AG-348 (mitapivat), an allosteric activator of red blood cell pyruvate kinase, increases enzymatic activity, protein stability, and ATP levels over a broad range of PKLR genotypes. *Haematologica*. 2021;106(1):238-249.
36. Kung C, Hixon J, Kosinski PA, et al. AG-348 enhances pyruvate kinase activity in red blood cells from patients with pyruvate kinase deficiency. *Blood*. 2017;130(11):1347-1356.
37. Smith LM, Kelleher NL; Consortium for Top Down Proteomics. Proteoform: a single term describing protein complexity. *Nat Methods*. 2013;10(3):186-187.
38. Huang A, Huang C, Zhang M, Zhu X, Qin X. Analysis of glycosylation profiles of serum glycoprotein from iron overload thalassemia. *Clin Lab*. 2018;64(7):1279-1287.
39. Kahane I, Ben-Chetrit E, Shifter A, Rachmilewitz EA. The erythrocyte membranes in beta-thalassemia. Lower sialic acid levels in glycophorin. *Biochim Biophys Acta*. 1980;596(1):10-17.
40. Talasz H, Sarg B, Lindner HH. Site-specifically phosphorylated forms of H1.5 and H1.2 localized at distinct regions of the nucleus are related to different processes during the cell cycle. *Chromosoma*. 2009;118(6):693-709.
41. Happel N, Stoldt S, Schmidt B, Doenecke D. M phase-specific phosphorylation of histone H1.5 at threonine 10 by GSK-3. *J Mol Biol*. 2009;386(2):339-350.
42. Sharma K, D'Souza RC, Tyanova S, et al. Ultradeep human phosphoproteome reveals a distinct regulatory nature of Tyr and Ser/Thr-based signaling. *Cell Rep*. 2014;8(5):1583-1594.
43. Boeing S, Williamson L, Encheva V, et al. Multiomic analysis of the UV-induced DNA damage response. *Cell Rep*. 2016;15(7):1597-1610.
44. Kettenbach AN, Schweppe DK, Faherty BK, Pechenick D, Pletnev AA, Gerber SA. Quantitative phosphoproteomics identifies substrates and functional modules of Aurora and Polo-like kinase activities in mitotic cells. *Sci Signal*. 2011;4(179):rs5.
45. Peng S, Zhao S, Yan F, et al. HDAC2 selectively regulates FOXO3a-mediated gene transcription during oxidative stress-induced neuronal cell death. *J Neurosci*. 2015;35(3):1250-1259.
46. Zhao K, Liu JF, Zhu YX, et al. Hemgn protects hematopoietic stem and progenitor cells against transplantation stress through negatively regulating IFN-gamma signaling. *Adv Sci (Weinh)*. 2022;9(5):e2103838.
47. Tsai SC, Seto E. Regulation of histone deacetylase 2 by protein kinase CK2. *J Biol Chem*. 2002;277(35):31826-31833.
48. Woo SH, An S, Lee HC, et al. A truncated form of p23 down-regulates telomerase activity via disruption of Hsp90 function. *J Biol Chem*. 2009;284(45):30871-30880.
49. Lees-Miller SP, Anderson CW. Two human 90-kDa heat shock proteins are phosphorylated in vivo at conserved serines that are phosphorylated in vitro by casein kinase II. *J Biol Chem*. 1989;264(5):2431-2437.
50. Chen L, Brown JW, Mok YF, Hatters DM, McKnight CJ. The allosteric mechanism induced by protein kinase A (PKA) phosphorylation of dematin (band 4.9). *J Biol Chem*. 2013;288(12):8313-8320.
51. Tang HY, Speicher DW. In vivo phosphorylation of human erythrocyte spectrin occurs in a sequential manner. *Biochemistry*. 2004;43(14):4251-4262.
52. Yamaguchi T, Nakano T, Matsumoto M, Terada S. Effects of chemical modification of cysteines 201 and 317 of band 3 on hemolytic properties of human erythrocytes under hydrostatic pressure. *Jpn J Physiol*. 1998;48(3):205-210.
53. Vallese F, Kim K, Yen LY, et al. Architecture of the human erythrocyte ankyrin-1 complex. *Nat Struct Mol Biol*. 2022;29(7):706-718.
54. Franco SS, De Falco L, Ghaffari S, et al. Resveratrol accelerates erythroid maturation by activation of FoxO3 and ameliorates anemia in beta-thalassemic mice. *Haematologica*. 2014;99(2):267-275.
55. De Franceschi L, Bertoldi M, De Falco L, et al. Oxidative stress modulates heme synthesis and induces peroxiredoxin-2 as a novel cytoprotective response in B-thalassemic erythropoiesis. *Haematologica*. 2011;96(11):1595-1604.
56. Papoin J, Yan H, Leduc M, et al. Phenotypic and proteomic characterization of the human erythroid progenitor continuum reveal dynamic changes in cell cycle and in metabolic pathways. *Am J Hematol*. 2024;99(1):99-112.
57. van de Wetering C, Manuel AM, Sharafi M, et al. Glutathione-S-transferase P promotes glycolysis in asthma in association with oxidation of pyruvate kinase M2. *Redox Biol*. 2021;47:102160.
58. Sarg B, Helliger W, Talasz H, Forg B, Lindner HH. Histone H1 phosphorylation occurs site-specifically during interphase and mitosis: identification of a novel phosphorylation site on histone H1. *J Biol Chem*. 2006;281(10):6573-6580.
59. Takagi M, Nishiyama Y, Taguchi A, Imamoto N. Ki67 antigen contributes to the timely accumulation of protein phosphatase 1gamma on anaphase chromosomes. *J Biol Chem*. 2014;289(33):22877-22887.
60. Eom GH, Cho YK, Ko JH, et al. Casein kinase-2alpha1 induces hypertrophic response by phosphorylation of histone deacetylase 2 S394 and its activation in the heart. *Circulation*. 2011;123(21):2392-2403.
61. Feng B, Jiao P, Helou Y, et al. Mitogen-activated protein kinase phosphatase 3 (MKP-3)-deficient mice are resistant to diet-induced obesity. *Diabetes*. 2014;63(9):2924-2934.
62. Husain-Chishti A, Faquin W, Wu CC, Branton D. Purification of erythrocyte dematin (protein 4.9) reveals an endogenous protein kinase that modulates actin-bundling activity. *J Biol Chem*. 1989;264(15):8985-8991.
63. Karur VG, Lowell CA, Besmer P, Agosti V, Wojchowski DM. Lyn kinase promotes erythroblast expansion and late-stage development. *Blood*. 2006;108(5):1524-1532.



64. Beneduce E, Matte A, De Falco L, et al. Fyn kinase is a novel modulator of erythropoietin signaling and stress erythropoiesis. *Am J Hematol*. 2019;94(1):10-20.
65. Karayel O, Xu P, Bludau I, et al. Integrative proteomics reveals principles of dynamic phosphosignaling networks in human erythropoiesis. *Mol Syst Biol*. 2020;16(12):e9813.
66. Seranova E, Connolly KJ, Zatyka M, et al. Dysregulation of autophagy as a common mechanism in lysosomal storage diseases. *Essays Biochem*. 2017;61(6):733-749.
67. Lupo F, Tibaldi E, Matte A, et al. A new molecular link between defective autophagy and erythroid abnormalities in chorea-acanthocytosis. *Blood*. 2016;128(25):2976-2987.
68. Zhang X, Campreciós G, Rimmelé P, et al. FOXO3-mTOR metabolic cooperation in the regulation of erythroid cell maturation and homeostasis. *Am J Hematol*. 2014;89(10):954-963.
69. Zhang S, Macias-Garcia A, Velazquez J, Paltrinieri E, Kaufman RJ, Chen JJ. HRI coordinates translation by eIF2alphaP and mTORC1 to mitigate ineffective erythropoiesis in mice during iron deficiency. *Blood*. 2018;131(4):450-461.
70. Sharapov MG, Novoselov VI, Penkov NV, et al. Protective and adaptogenic role of peroxiredoxin 2 (Prx2) in neutralization of oxidative stress induced by ionizing radiation. *Free Radic Biol Med*. 2019;134:76-86.
71. Toya MSC MA, Federti E, Perduca M, et al. The novel role that Nrf2 plays in erythropoiesis during aging. *Blood*. 2019;134(suppl 1):3502.
72. Zhang H, Gong W, Wu S, Perrett S. Hsp70 in redox homeostasis. *Cells*. 2022;11(5):829.
73. Fibach E, Rachmilewitz EA. The two-step liquid culture: a novel procedure for studying maturation of human normal and pathological erythroid precursors. *Stem Cells*. 1993;11(suppl 1):36-41.
74. Hennrich ML, Romanov N, Horn P, et al. Cell-specific proteome analyses of human bone marrow reveal molecular features of age-dependent functional decline. *Nat Commun*. 2018;9(1):4004-4021.
75. De Franceschi L, Ronzoni L, Cappellini MD, et al. K-CL co-transport plays an important role in normal and beta thalassemic erythropoiesis. *Haematologica*. 2007;92(10):1319-1326.